15 Aug 2008, 8:00 am - 8:30 am

Analysis of Two Case Histories of Violent Landslides Triggered by Earthquakes

N. Gerolymos

National Technical University, Athens, Greece/ Iroon Politechniou, Athens, Greece

6th International Conference on
Case Histories in Geotechnical Engineering, Arlington, VA, August 11-16, 2008

ANALYSIS OF TWO CASE HISTORIES OF VIOLENT LANDSLIDES TRIGGERED BY EARTHQUAKES

N. Gerolymos
National Technical University, Athens, Greece
Iroon Politechniou, Athens–Greece 15780

ABSTRACT

Two earthquake–triggered violent landslides are studied. The Nikawa, activated by the M_w 7 1995 Kobe Earthquake, and the Higashi–Takezawa, activated by the M_{JMA} 6.8 2004 Niigata-ken Chuetsu earthquake, in Japan. Both landslides involved about 100 m displacement of a large wedge of an originally rather mild slope. The surprisingly large and rapid in nature runoff of the soil masses, motivated several researchers to interpret the sliding process. There is still no consensus as to which were the actual causes of those two catastrophic events. The goal of the paper is to study: (i) the landslide triggering and propagation, and (ii) the mechanism of material softening inside the shear band responsible for the accelerating movement of the two slides. To this, a model is utilised considering two mechanically coupled substructures: (a) the accelerating deformable body of the slide, and (b) the rapidly deforming shear band at the base of the slide. It combines features of an extended Savage–Hutter approach, with (a) Mohr–Coulomb failure criteria, and (b) Bouc–Wen hysteretic stress–strain relationship, and exploits the concept of grain crushing–induced instability. The method successfully interprets the studied landslides.

THE CASE STUDY OF NIKAWA LAND-SLIDE, JAPAN (1995)

Introduction

The M_w7 1995 Kobe Earthquake was one of the few major earthquakes to directly hit a sophisticated modern city possessing an extremely high concentration of civil engineering facilities. It resulted in the worst earthquake-related disaster in Japan since the 1823 M_s8 Kanto earthquake. The port of the city, of critical importance to the Japanese economy, was left almost completely out of service, while very significant was the damage to the elevated highways which carried the traffic through the city. See the numerous detailed reports by the Japanese Geotechnical Society, 1996; Committee of Earthquake Engineering, 1996; Earthquake Engineering Research Institute, 1995.

Through all this tremendous devastation on all types of engineered structures, the nearly 400 landslides that also took place did not catch the attention of the casual observer (Sassa et al. 1996). Most of them were of relatively small size, often associated with tensile cracking, and of limited motion–-not unexpectedly in view of the fact that the earthquake occurred in the "dry" season. A conspicuous exception was the Nikawa rapid landslide — one of the most devastating landslides directly related to an earthquake (Figs 1 and 2). With a landslide volume in the order of 110,000 m^3 (Sassa et al., 1996), moving

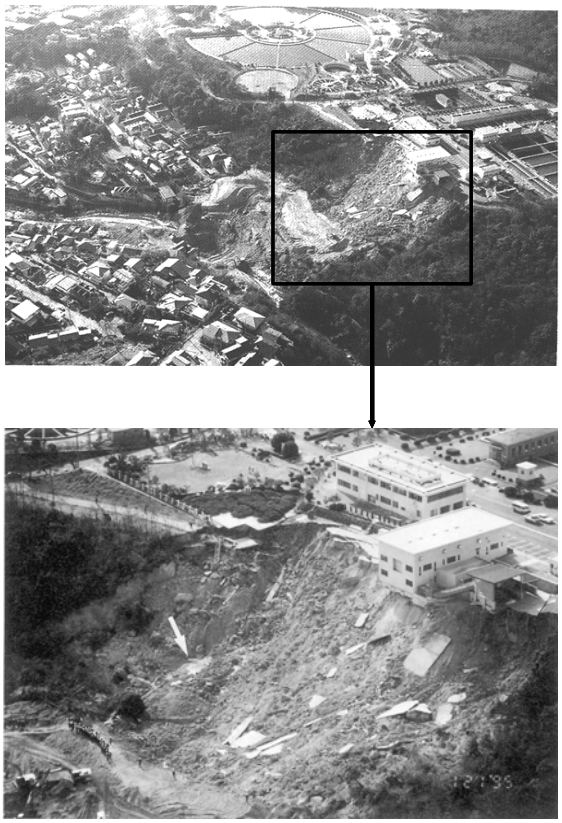

Fig. 1. The Nikawa landslide: aerial photos [Sassa et al, 1996]

in just a few seconds over a distance of more than 100 m, it destroyed 11 residential buildings causing 35 fatalities. In addition of course to strong seismic shaking perhaps accentuated by topographic amplification (Kalou & Gazetas, 2001), several deeper causes, such as "sliding-surface liquefaction" (Sassa, 1995) and water-"film" generation (Kokusho, 2000), have been proposed to explain rapid runoff of the slide.

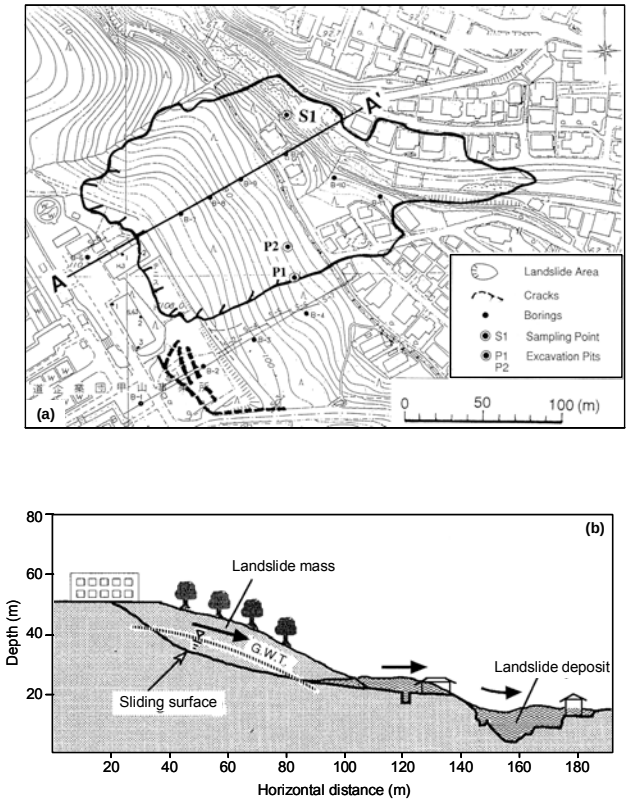

Fig. 2. The Nikawa landslide : (a) plan view, and (b) cross section [Sassa et al, 1996]

Earthquake Characteristics and Ground Shaking

At 17:46 on January 17 1995, the Hyogo-Ken Nanbu earthquake with a magnitude M_{JMA} = 7.2, struck Kobe and seriously damaged infrastructures, triggered landslides, and causes many deaths and injuries. The losses were estimated to about $200 billions. The mechanism of the earthquake was a strike–slip fault, dipping 77 degrees and striking N229E (Sato, 1996). The number of recorded aftershocks were more than 6000 with the largest one equal to M_{JMA} = 4.9 that occurred within two hours after the mainshock .

The recorded Peak Ground Acceleration (PGA) reached 0.60 g at level ground very close to Nikawa. The very small distance from the NE part of the causative fault can explain such a large PGA. The combination of soil and topographic amplification could have played a major role, at least in triggering the landslide. In such a case, basic free–field motion could have possibly been amplified at the sliding mass. With such an excitation, the developing shear stresses could possibly lead to liquefaction of even marginally sensitive soil layers. However, even if such a triggering-related mechanism were true the 140 m displacement could not be anticipated.

Geometry, Geology, Groundwater and Soil Properties

The earthquake took place during a dry season, which followed a historically–dry 1994 summer. The limited amount of rainfall possibly played a major role in reducing the number of landslides triggered by the earthquake. The most important landslides (such as Nikawa) were associated with the so–called Osaka Group layers, that consisted of limnic and marine deposits of sands and clays from Pliocene to Middle Pleistocene, with low permeability. Within these fairly impermeable layers, pore water could have been preserved despite the dry season. Therefore, while most landslides originated within un-saturated soil and hence were of moderate magnitude engineers this was not the case with Nikawa. Engineers were surprised with the significant distance and speed of the runoff, because: (a) the slope inclination barely exceeded 20°, (b) the water table was not high (although there was evidence that it was above the sliding surface for a significant length), (c) the soil along the sliding surface consisted of rather dense coarse-grained sand to silty sand, material not readily susceptible to liquefaction. A typical grain size distribution of this soil is plotted in Fig. 3.

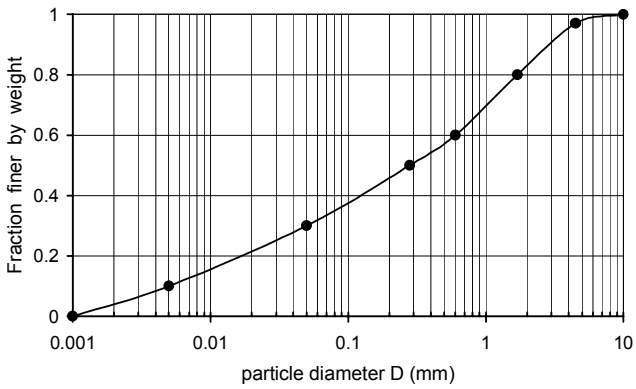

Fig. 3. Grain size distribution for blue granitic sand found at the bottom of the Nikawa landslide mass (Sassa et al. 1996). The initial potential for breakage B_{p0} is equal to 0.72.

As depicted in the geotechnical cross-section of Fig. 4, the slope of the landslide mass did not exceed 20°. The number of blows of the standard penetration test, N_{SPT}, ranged from 10 (near the surface) to 60 (refusal, in the Japanese scale). Secondary sedimentary layers and terrace layers were found to overly the Osaka group (granitic sand and clay). The bedrock granite was detected at 25 m (borehole B9) to 35 m depth (borehole B6). The apparent residual friction angle of the shear band material was measured to be $\varphi_a \approx 8.5°$ (compared to the drained residual friction angle $\varphi \approx 30°$). Several wit-

nesses asserted that water was flowing from the base of the landslide the very next day.

Possible Causes or Contributing Factors

The extent of the runoff along with its rapid nature, which left no time for response, led Sassa et al. (1996) in developing a hypothesis which he called *"sliding-surface liquefaction"*. As depicted in Fig. 5, in the conventional liquefaction the strength loss is associated with pore pressure buildup, due to the tendency of the soil to contract when subjected to shearing. Sliding surface liquefaction is quite different: when the soil is subjected to shearing, and after a sliding surface has been developed, the crushing of sand grains and the consequent increase in volume of solids is the mechanism of pore pressure buildup, leading to a different type of "liquefaction". Sassa and coworkers developed a high-speed ring-shear apparatus to test soil specimens from Nikawa, with shearing speeds in the order of 0.3 m/s. While in conventional liquefaction the pore pressure buildup is rapid, these tests showed a gradual increase of pore pressure and a subsequent drop of the apparent friction angle to about 8.5°, without any sign of liquefaction in the sample. The grain crushing became evident from the grain size distribution along the shear zone.

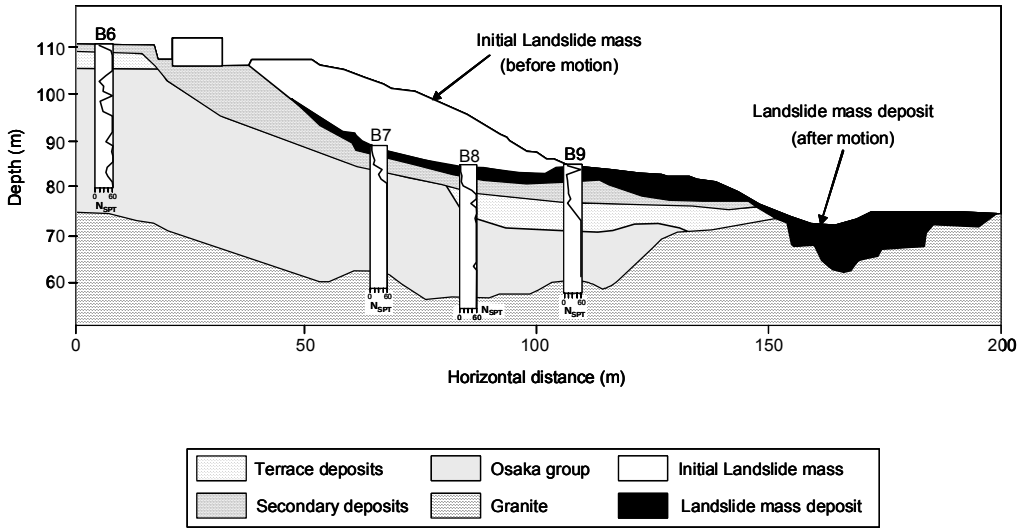

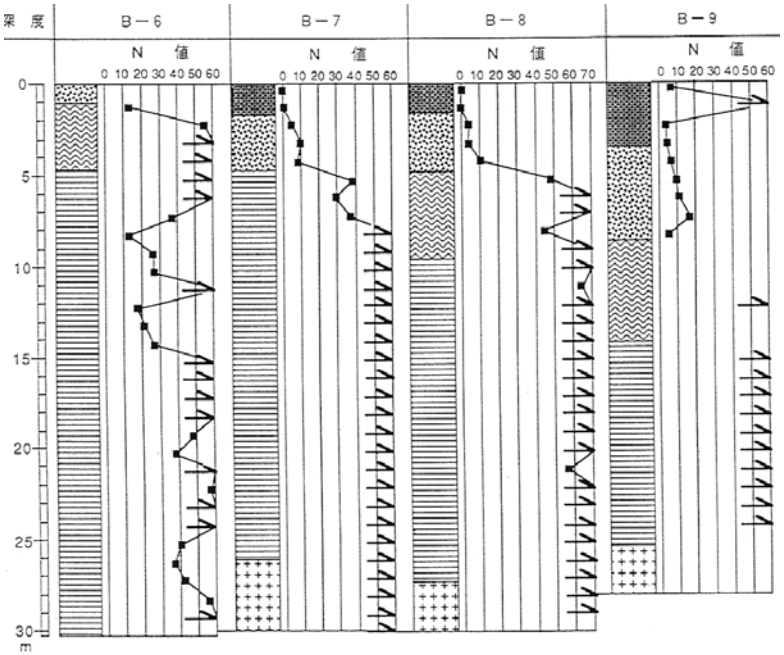

Fig. 4. Geotechnical cross section, along with NSPT blows on boreholes that were conducted after the slide [courtesy of Professor K. Sassa]

Some other alternative mechanisms can be invoked to explain the phenomenon. For instance, the mechanism of gradual "smoothing" of the sliding surface was proposed by Kokusho [2000] (not for Nikawa): it supposes that when a soil layer of significant thickness underneath the sliding surface liquefies, and the soil directly on top is impermeable (both conditions might apply in Nikawa), then the natural tendency of the liquefied layer to settle could produce a very slim "film" of water, only a few centimeters or even milimiters in thickness. The consequence of the appearance of this water film along the sliding surface could explain the extent of the runoff (about 100 m). However, the nature of the soils does not support such a theory.

THE CASE STUDY OF HIGASHI–TAKEZAWA LANDSLIDE, JAPAN (2004)

Introduction

The devastating 2004 Niigata–Ken Chuetsu earthquake (M_w 6.8) triggered 374 landslides more than 50 m wide (Sassa et al., 2005) 12 of which with volume larger than one million cubic meters. Among these landslides, Higashi–Takezawa was one of the largest. The landslide mass filled a valley and stopped a river flow forming a large natural reservoir (Fig. 6). It is believed, however, that the heavy rainfall during the last three days before the earthquake was a significant contributor to the triggering of those landslides (Sassa, 2005; Tsukamoto and Ishihara, 2005).

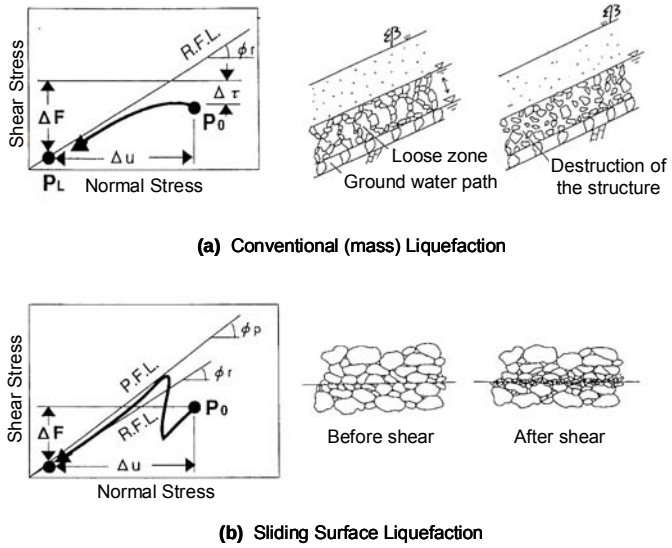

Fig. 5. (a) Conventional (mass) liquefaction, compared to (b) sliding surface liquefaction, in terms of the mechanism and the associated stress paths. (R.F.L. : Residual Failure Line, P.F.L. : Peak Failure Line) [Sassa, 1996].

The surprisingly large and rapid runoff of the soil mass motivated several researchers (Kokusho and Ishizawa, 2005; Tsukamoto and Ishihara, 2005; Sassa et al., 2005) to study the Higashi–Takezawa landslide, providing different interpretations of the sliding process. The questions to be answered arose on: (a) the exact position of the sliding surface, and (b) the mechanism of material softening behind the accelerating landslide movement. It is pointed out, that laboratory tests on soil samples taken from the site of the slip surface indicated undrained friction angles larger than the slip inclination (Sassa et al., 2005). Moreover, the sliding material consisting of silt to dense silty sand was not susceptible to liquefaction (Kokusho and Ishizawa, 2005).

In an effort to address the complex issue of triggering and post–failure travel distance of the landslide, Tsukamoto and Ishihara (2005) performed a series of drained triaxial tests on partially saturated sand samples taken from Higashi–Takezawa. Motivated by the reasonable assumption that rapid landslides would take place under conditions of little or practically no volume change, they followed a test procedure which is as follows: First, the non–saturated soil specimen is prepared with the wet tamping method. Then, it is consolidated through the application of confining stress and is loaded axially following a strain–controlled procedure. The volume change of the specimen is monitored during the phase of axial loading. Since the soil generally tends to decrease its volume during the early stages of shearing, the cell pressure is appropriately reduced to keep the volume of the specimen unchanged. This reduction is maintained until the cell pressure becomes equal to zero, and the test is continued until the axial strain reaches 10%.

Fig. 6. The Higashi–Takezawa landslide (source: Sassa et al, 2005)

Three tests were performed on specimens consolidated to a confining pressure σ_3 = 98 kPa with relative density D_r between 30 % to 35% and water content w = 10, 20 and 49 % (full saturation, S_r = 100%). The measured stress paths were found to be similar to those of conventional (mass) liquefaction. However, the friction angles were calculated to be as large as 65° to 75° (with larger values corresponding to higher water contents), do not justify such a mechanism of pore–pressure generation.

Figure 7 depicts the residual strength curve with respect to the water content. Interestingly the residual strength, defined as half of the deviatoric stress at large strains, is a decreasing function of water content. Indeed, there is a threshold limit of the water content, at w ≈ 25 %, below which no reduction of the residual strength is observed. For water content between 25% and 49% (full saturation), the residual strength reduces sharply with increasing water content. Finally, for water content greater than that corresponding to full saturation, the residual strength remains constant.

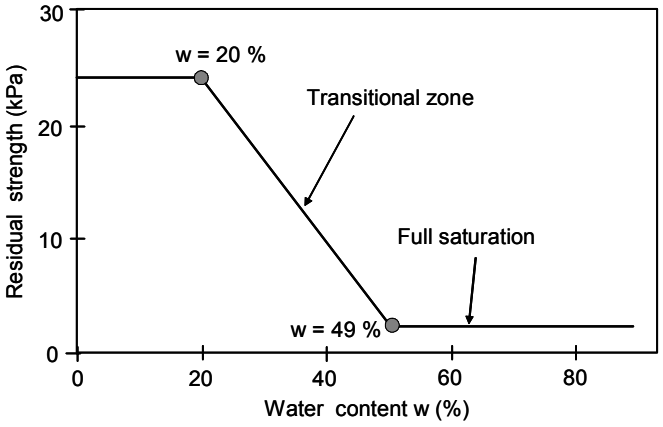

Fig. 7. Idealized plot of residual strength of the Higashi–Takezawa sand against water content (source: Tsukamoto and Ishihara, 2005)

The drained triaxial test under conditions of no volume change provides valuable information about the residual strength of un–saturated sand, which can be readily applied for the analysis of rapid landslide. Nevertheless, it has the following drawback: The residual strength is not the physical result of a pore–pressure generation mechanism. It is derived artificially through an imposed reduction of the cell pressure under the condition of zero volumetric strain rate.

After a detailed field survey of the head scarp of the Higashi–Takezawa landslide, Sassa et al. (2005) concluded that the sliding surface could have been formed within either the weathered (due to the existence of groundwater flow) top part of the outcropped siltstone layer, or the bottom of the overlain sand layer which was probably a part of previously moved landslide mass. Ring shear tests conducted by Sassa et al. (2005) on soil specimens taken from the sliding surface revealed that the residual friction angle of the silt was by far smaller than that of the sand, and close to the inclination angle of the slip plane. Neither of them could explain the rapid and large displacement of the landslide. However, the sand was found to be susceptible to grain–crushing induced softening.

Earthquake Characteristics and Ground Shaking

At 17:56 on October 2004, the Niigata–Ken Chuetsu earthquake with a magnitude M_{JMA} = 6.8, struck central Niigata-ken (Chuetsu area) and seriously damaged infrastructures of hilly and mountainous areas including Kawagushi town, Ojiya city, Nagaoka city, and their environs. The earthquake was an epicentral thrust–fault earthquake with a hypocenter of about 10 Km depth (Toyota et al., 2006). The main shock was followed by three major aftershocks with M_{JMA} equal or larger than 6.0 that occurred within one hour after. In addition, several other subsequent aftershocks continued for about two weeks (Koseki et al., 2006).

The actual seismic excitation exerted on the landslide cannot be known in detail, as it is influenced by many parameters such as the geology, topography, site conditions and distance from the fault. Nevertheless, the nearest (to the landslide) observation station NIG019 at Ojiya, around 10 Km west of the Higashi–Takezawa landslide and WNW 7 km from the epicenter of the main shock, recorded acceleration time histories characterized by peak values of PGA = 1.3 g (Sassa et al. 2005).

Geometry and Kinematics

The main body of the landslide is indicated in the plan of Fig. 8 deduced from an air borne laser scanning survey carried out three days after the earthquake (Sassa et al., 2005). A cross–section of the landslide is also depicted in Fig. 8. The gentle slope inclination before the failure suggested that the landslide was probably a reactivation of an earlier one. The landslide involved a soil volume of about 1,200,000 m^3 (Kokusho and Ishizawa, 2005). The maximum dimensions in plan were about 300 m width and 250 m length, and the maximum thickness was about 40 m (Kokusho and Ishizawa, 2005, Sassa et al., 2005). The landslide mass moved rapidly about 100 m, and hit the opposite bank of Imokawa river. One part of the sliding mass spread across the road and hit a school. From the head scarp of the landslide, consisting of a rather impermeable stiff siltstone, the inclination angle of the sliding surface was estimated by the aforementioned authors to be approximately 20^o.

Geology, Groundwater and Soil Properties

A schematic geological section of the landslide area is shown in Fig 8. The subsoil is a Neogene formation, consisting of sandstone (the main body of the landslide) underlain by siltstone. The terrace along the river and below the toe of the landslide consists of marine sand from the Tertiary period. The groundwater flow over the siltstone layer, lead Sassa et al. (2005) to assume the existence of a thin silt layer between the sandstone and the siltstone, due to the unavoidable weathering of the siltstone. Although, this silt layer was not detected at the head scarp, the assumption of Sassa et al. (2005) was reinforced from field investigation of the head scarp of the nearby

Terrano landslide located also near river Immokawa. The Terrano landslide, triggered by the Niigata–Ken Chuetsu earthquake, had the same subsoil and groundwater conditions. The silt encountered at the head scarp of the Terrano landslide was weathered and soft.

Water seepage observed on the head scarp of the landslide three days after the earthquake suggests that the water table was located well above the sliding plane. No precipitation occurred for three-four days before the earthquake, but heavy rains had occurred the weeks before.

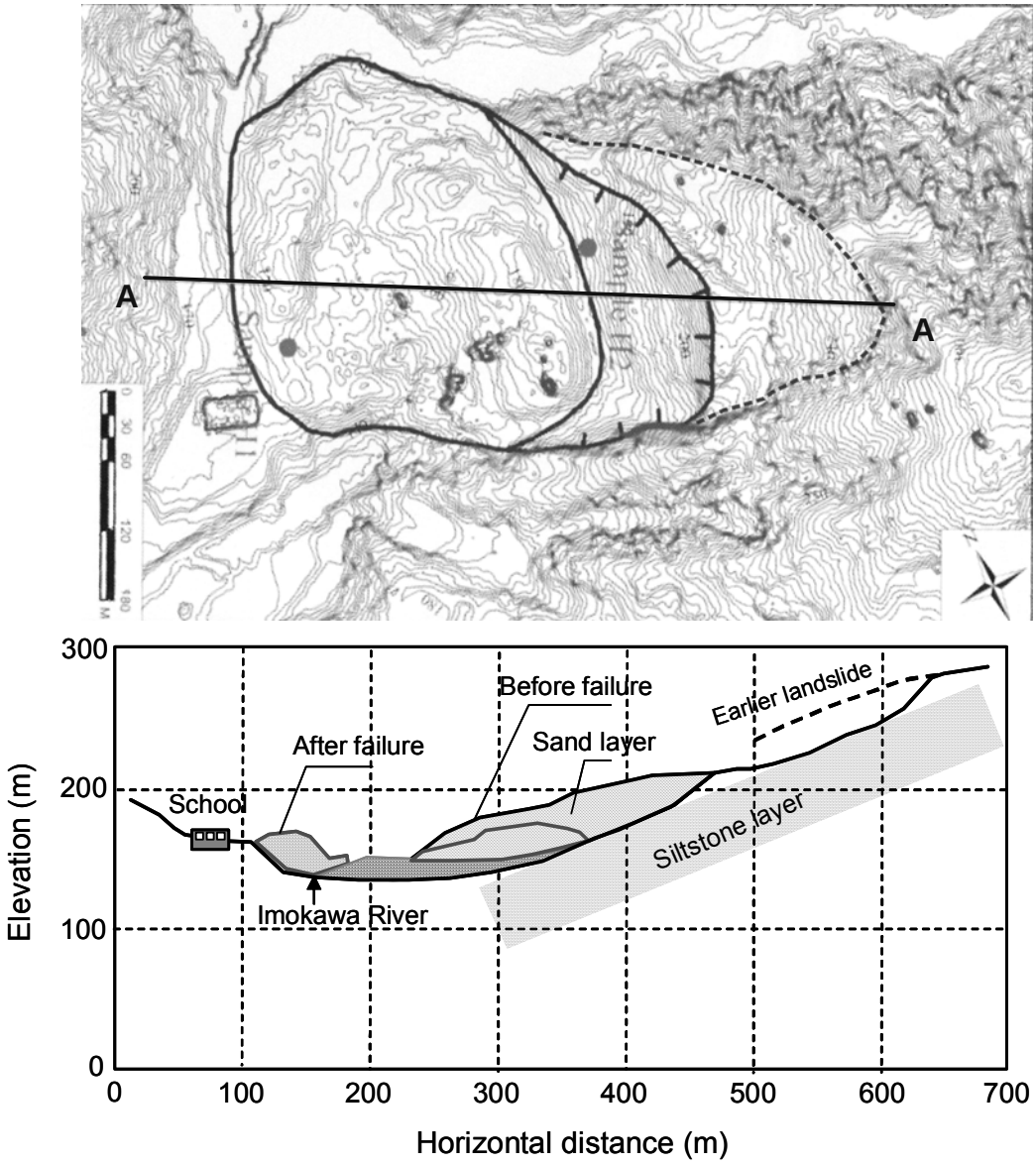

Fig. 8. The Higashi–Takezawa landslide: (a) plan view, and (b) cross section (based on information by Sassa et al., 2005)

The grain size distribution of the sand involved in the sliding surface of the Higashi–Takezawa landslide is illustrated in Fig. 9, along with that of the Terrano silt which is considered to be representative of the Higashi–Takezawa silt. The strength properties of the soils under consideration were obtained from consolidated–drained and undrained high speed ring shear tests (Sassa et al., 2005). The undrained friction angle of the sand was found to be 37^{o}, while the residual friction angle of the Terrano silt was 24^{o}. However, one peculiar aspect of the Higashi–Takezawa sand is its mechanical instability due to grain crushing. Indeed, the cyclic loading test, resulting in an apparent residual friction angle of merely 3.3^{o}, strongly suggesting that the Higashi–Takezawa sand is susceptible to grain crushing–induced instability.

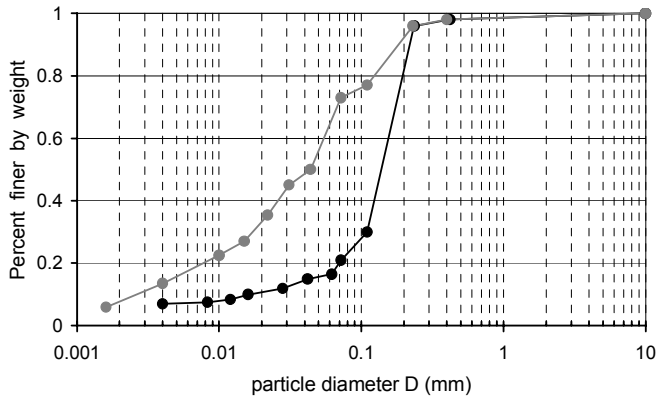

Fig. 9. Grain size distribution of the Higashi–Takezawa sand (black line) and Terrano silt (gray line), after Sassa et al. (2005)

THE MODEL : EQUATIONS AND PARAMETERS

Problem Definition

The problem studied is that of a finite moving soil mass assembled by a number of columns in contact with each other (Fig. 10). The columns are free to deform but retain fixed volumes (constant density ρ_s) of solid–fluid mixtures during their movement down a slope. The evolution of the mixture is considered to be one–dimensional with no aggradation or degradation processes and with uniformly–distributed (depth–integrated) velocity along each column. At the base of the sliding mass we assume a shear band of infinite length and of zero thickness.

The field variables are the thickness of the landslide h, excess pore water pressure p, the breakage potential B_p, and the relative velocity υ between top and bottom. The velocity is considered to increase linearly with the distance from the bottom of the shear band, from zero to the maximum value υ at the top of the shear band. The breakage potential B_p is a measure of the evolution of the particle size distribution curve with loading, as defined in the sequel. It is pointed out that the parameter B_p is the current value of the breakage potential, and should not be confused with that originally defined by Hardin (1985), denoted as B_{p0}. The latter, B_{p0}, is the initial (i.e. before loading) breakage potential, and is a constant.

Applying the mass and momentum conservation laws and using Eulerian description of motion, a system of two partial differential equations are obtained:

$$\frac{\partial h}{\partial t} + \upsilon \frac{\partial h}{\partial x} + h \frac{\partial \upsilon}{\partial x} \tag{1}$$

and

$$\frac{\partial (h \bar{\sigma}_x)}{\partial x} + T_d - T_r - T_f = \rho_s h \left(\frac{\partial \upsilon}{\partial t} + \upsilon \frac{\partial \upsilon}{\partial x} + \frac{d \upsilon_g}{dt} \right) \tag{2}$$

h is the thickness in the z direction normal to the bed, υ is the depth–averaged velocity in the x direction parallel to the base of the landslide, υ_g is the seismic velocity imposed at the base of the landslide parallel to the dip direction of the sliding surface, T_d is the gravitational driving force acting on the landslide mass, T_r is the resisting force due to hysteretic (Coulomb) friction at the bed influenced by bed curvature (Gray et al. 1999; Iverson and Delinger 2001; Pudasaini and Hutter, 2003); It is a function of τ_m the cyclic shear resistance mobilized along the shear band. A detailed description of this term will be provided below; and T_f the turbulent resisting force at the base of the slide, represented by the quadratic Chezy constitutive law.

In Eqn (2), $\bar{\sigma}_x$ is the average – along the depth of the sliding mass – longitudinal normal stress due to elongation or compression of the soil mass in the x direction. The longitudinal normal stress is assumed to be a combination of a lithostatic (depth–dependent) term and a strain rate dependent term

$$\bar{\sigma}_x = \frac{1}{2} \left(K - \eta_d \frac{\partial \upsilon}{\partial x} \right) \rho_s g h \cos\theta \tag{3}$$

in which K is the lateral earth pressure coefficient at rest, and η_d is a viscous coefficient that controls the transition from the active ($\partial \upsilon / \partial x > 0$) to the passive ($\partial \upsilon / \partial x \le 0$) state, depending on whether a soil column is expanding or contracting. For the special case of $K = 0$ and $\eta_d = 0$, the sliding mass behaves as a rigid body and Eqn (2) vanishes to the well known Newmark (1965) sliding block model.

Equations for Frictional Behaviour

A versatile one–dimensional constitutive model is utilised to describe the shear stress–displacement relationship inside the shear band. The model is capable of reproducing an almost endless variety of stress–strain forms, monotonic as well as cyclic. Based on the original proposal by Bouc (1971) and Wen (1976), the model was recently extended by Gerolymos and Gazetas (2005) and applied to cyclic response of soils and earthquake–triggered rapid landslides (Gerolymos et al., 2007; Gerolymos and Gazetas, 2007a; 2007b). It is used herein in conjunction with a Mohr–Coulomb friction law and Terzaghi's effective stress principle.

The mobilized shear stress inside the shear band is expressed as:

$$\tau_m = \tau_y \zeta \tag{4}$$

where τ_y is the ultimate shear strength, which is a function of time. The parameter ζ is a hysteretic dimensionless quantity,

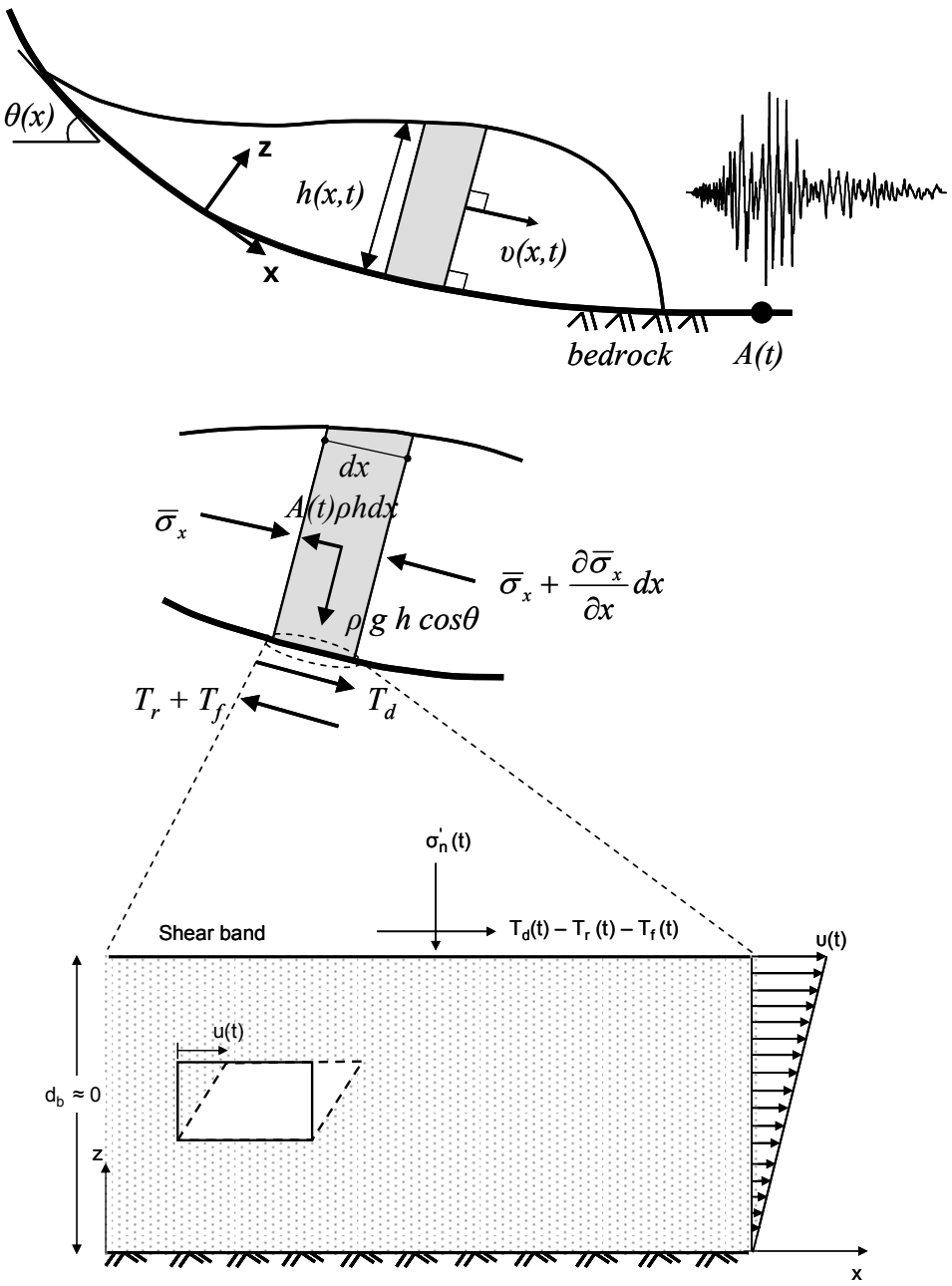

Fig. 10. 1 dimensional depth–integrated model for the analysis of earthquake–induced landslide evolution. Stress equilibrium is referenced to a local coordinate system that is fitted to the underlying topography.

controlling the nonlinear response of the soil. It is governed by the following differential equation:

$$\frac{d\zeta}{du} = \frac{1}{u_y}\left\{1 - |\zeta|^n \left[b + (1-b)\,\mathrm{sgn}(\upsilon\zeta)\right]\right\} \tag{5}$$

in which u_y , n and b, are parameters that control the shape of the shear stress versus displacement curve. The parameter τ_y is defined as:

$$\tau_y = \mu\left(\sigma'_{n0} - p\right) \tag{6}$$

in which the friction coefficient, μ, is expressed in terms of the Coulomb friction angle φ' of the soil in direct shear, σ'_{n0} is the initial effective normal stress, and p is the excess pore–water pressure, generated due to particle breakage.

Equations for Grain Crushing–Induced Pore–Water Pressure

The mechanism of pore–water pressure generation due to particle breakage is assumed to be governed by the following equation (Gerolymos and Gazetas, 2007a; 2007b):

$$\frac{\partial p}{\partial t} + \upsilon \frac{\partial p}{\partial x} = \frac{\partial}{\partial z}\left(c_v\left(B_p\right)\frac{\partial p}{\partial z} \right) - \lambda \frac{\partial B_p}{\partial t}\sigma'_{n0} \qquad (7)$$

in which B_p is the current value of the breakage potential; c_v and λ are the coefficients of consolidation and pore–pressure–breakage, respectively. Note that c_v is a function of B_p. In fact, c_v decreases with decreasing particle size and thus with particle crushing evolution.

This expression is being simplified in the limit of undrained loading conditions, which is a reasonable assumption when the shear band is deformed at a large velocity (rapid landslide). Parameter λ controls the ultimate value of the pore–water pressure.

Equations for Grain Crushing

The breakage potential B_p is a measure of the evolution of the particle size distribution curve with loading; it is indicative of the amount of grain crushing. A key assumption, motivated by scant experimental evidence is that the evolution of B_p with time is governed by the following equation (Gerolymos and Gazetas, 2007a):

$$\frac{dB_p}{dt} = \xi\left(B_{pl} - B_p\right) \qquad (8)$$

in which ξ is the coefficient of grain crushing; B_{pl} is the final (after loading) breakage potential relating to B_{p0}, the initial (before loading) value of the potential as defined by Hardin (1985), according to:

$$B_{pl} = \frac{B_{p0}}{1 + S^{n_b}} \qquad (9)$$

The definition of B_{p0} is schematically illustrated in Fig. 11. n_b is the crushing number (Hardin, 1985), S is the stress loading factor which is a function of the mobilized shear stresss τ_m, the effective normal stress σ'_n, the crushing hardness h_c ,shape number of the particle n_s, and the initial void ratio e_0 of the particles mixture (Hardin, 1985). Calibration of the model parameters is achieved through numerical simulations of undrained cyclic ring shear tests (Gerolymos and Gazetas, 2007a; 2007b).

For a given shear stress time history, Eqns (4), (5), (7), and (8) form a system of highly nonlinear partial differential equations with four unknowns: the excess pore–water pressure p, the breakage potential B_p, the hysteretic parameter ζ, and the displacement u.

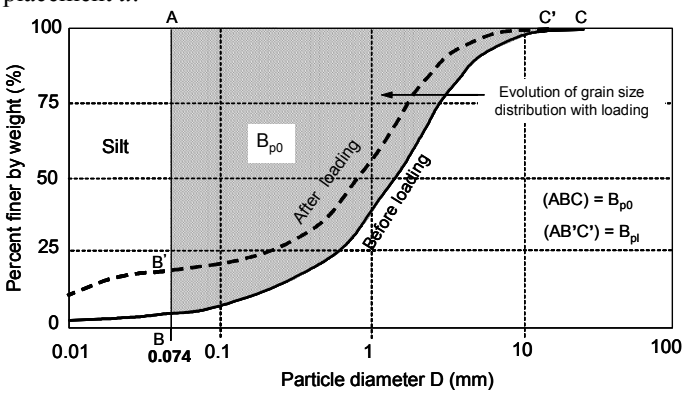

Fig. 11. Definition of the initial breakage potential B_{p0}, after Hardin (1985)

NUMERICAL ANALYSIS: RESULTS AND DISCUSSION

The Higashi Takezawa Landslide

With the developed model for seismic triggering and evolution of grain–crushing–induced landslide we analyse the case of Higashi–Takezawa . The seepage force is ignored, since the actual level of the water table during the earthquake is not known. Three scenarios are studied regarding the potential location of the sliding surface and the susceptibility of sand to grain crushing:

(a) The shear band formed within the sand layer (i.e., in the main body of the landslide), the sand is not susceptible to grain crushing, and the upper part of the siltstone is assumed to have remained intact.

(b) The shear band formed within an assumed thin silt layer atop the siltstone, but the sand is not susceptible to grain crushing.

(c) The shear band formed within the sand layer, the sand *is* susceptible to grain crushing, and the upper part of the siltstone is assumed to have remained intact.

The results of the analysis for cases (a) and (b) are shown comparatively in Fig. 12 in the form of time histories of relative shear displacement. The maximum computed displacement at the end of shaking for case (a) is 0.65 m, which is by far smaller than that of 3.4 m for case (b). These values of displacement suggest that the existence of a thin silt layer atop the siltstone is more crucial for triggering the landslide. However, none of those displacements could explain the observed rapid and large run-out distance of the landslide. It is therefore reasonable to assume that grain crushing–induced pore–pressures could be a major destabilizing factor for the landslide.

The results of the analysis for case (c) are presented in Figs 13–16 in terms of snapshots of the landslide evolution (Fig. 13), and distributions of velocity v (Fig. 14), excess pore–water pressure ratio r_u (Fig. 15), and breakage potential B_p (Fig. 16), along the sliding surface. The following observations are worthy of note regarding the response of the sliding wedge:

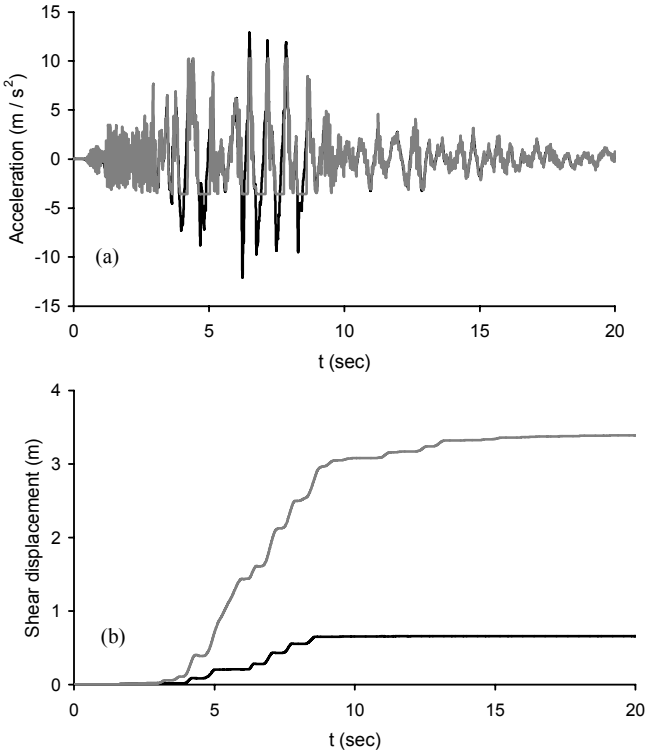

Fig. 12. (a) Input (Record NIG019 2004: PGA = 1.3 g) and response acceleration time histories at the base of the landslide (black line), and at the soil wedge (gray line) for case b (sliding surface within an assumed thin silt layer), and (b) computed time histories of relative shear displacements, for sliding surface: (i) within the sand layer (no grain crushing is considered, maxu = 0.65 m) (black line), and (ii) within an assumed thin silt layer at the top of the siltstone (maxu = 3.4 m) (gray line)

At the early stages of the seismic motion, excess pore water–pressure due to particle crushing is generated at the head of the wedge and propagates rapidly towards its toe. In the following few seconds the excess pore–water pressure ratio rises up very quickly reaching values larger than 0.9 along the entire length of the sliding surface (t = 12.5 sec). At this time, sliding originates at the head of the soil wedge, and landsliding begins. It is very interesting that triggering occurs almost at the end of seismic shaking, when the motion has essentially subsided, and not during the strong seismic shaking as one would expect. This implies that grain crushing–induced pore–pressure is a cumulative process and thus depends strongly on the history of loading.

After its initiation the landslide moves rapidly towards the riverbed, developing velocities between 5 m/s and 10 m/s. Velocities with smaller values concentrate on the rear of the landslide, while those with larger values are mostly at the front which essentially governs the "race" of the entire landslide. At t = 22.5 sec the sliding soil mass enters the riverbed while at this time the frontal part of the landslide detaches from the main body, spreads across the river, hits the opposite bank with a velocity of 16 m / s (at t = 26.5 sec), and finally reaches the school at t = 30 sec. Following this frenetic motion of the detached frontal part, the main body of the landslide accumulates inside the riverbed forming a natural reservoir which decelerates the trailing part of the landslide. The reduction in velocity begins at the rear and progressively shifts to the front.

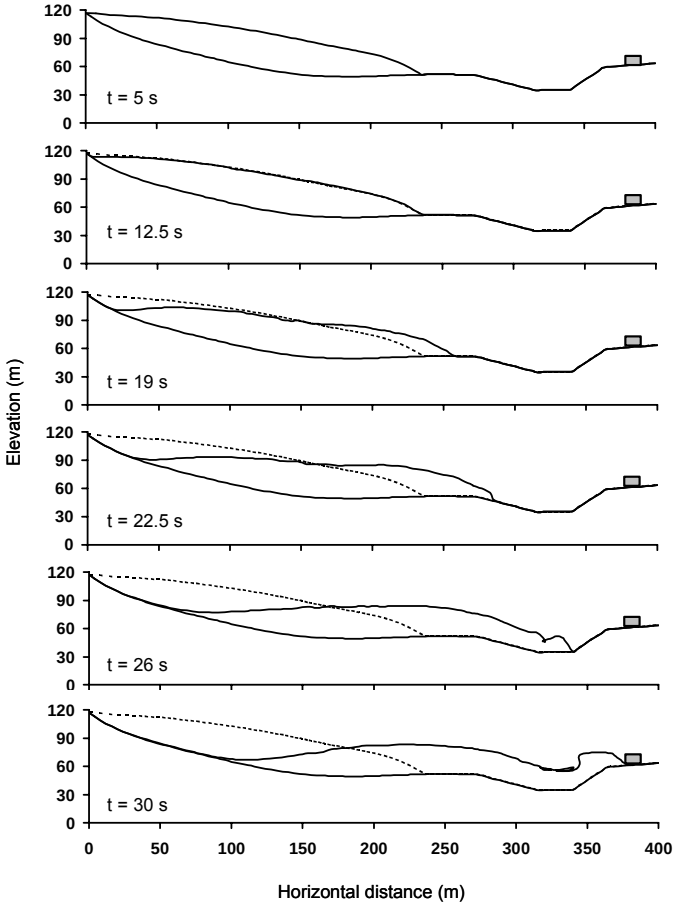

Fig. 13. Snapshots of the computed evolution of the Higashi–Takezawa landslide. The school is indicated with the gray box. The initial ground surface is shown as dotted line

It is seen that the calculated sliding process extended from the ruptured scrap in the source zone to the deposition fan on the riverbed and near the school, is consistent with the field observation (Sassa et al., 2005). Clearly, there are four major stages in the run-out process, namely, triggering (at t ≈ 12.5 sec), accelerating motion towards the riverbed (12.5 sec < t < 22.5 sec), separation of the frontal part from the main body of the landslide (at t = 22.5 sec), and deposition and deceleration (t > 22.5 sec).

To get an insight into the mechanics behind this disastrous response, Fig. 16 plots the evolution of particle breakage potential B_p. Notice that B_p approaches a steady state value of 0.30

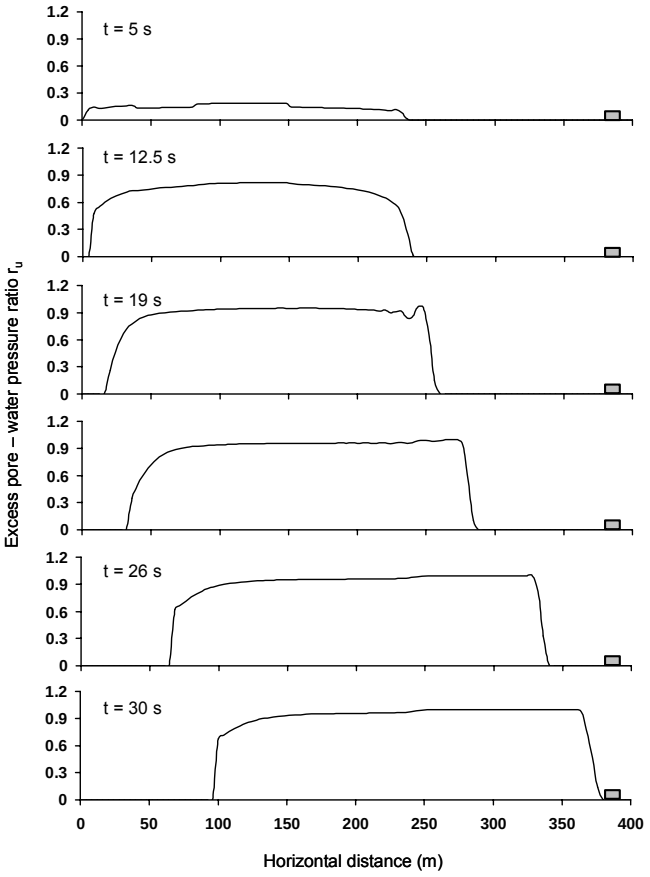

Fig. 14. Snapshots of the computed excess pore–water pressure ratio along the sliding surface for the Higashi–Takezawa landslide. The school is indicated with the gray box

at t > 15 sec; this is larger than the initial value of B_{pl} (computed to be 0.27 in drained loading conditions), reflecting the influence of the developed excess pore–water pressures. The slightly increasing breakage potential at t > 15 sec reveals that the grain crushing process has been practically terminated. The effective normal stress is not adequate for further breakage. However, the landslide is still accelerating due to the action of gravity.

The Nikawa Landslide

The developed model for landslide kinematics was also applied to analyse the case of Nikawa. The response of the potentially sliding wedge is summarized in Figs 17 to 19. Specifically:

Figure 17 plots snapshots of the landslide evolution. The speed of sliding picks up dramatically after the triggering of the landslide at approximately t = 14 sec, approaching values of about 13 m/s at the end of shaking (Fig. 18). All that is needed for a huge displacement to develop is time. During the

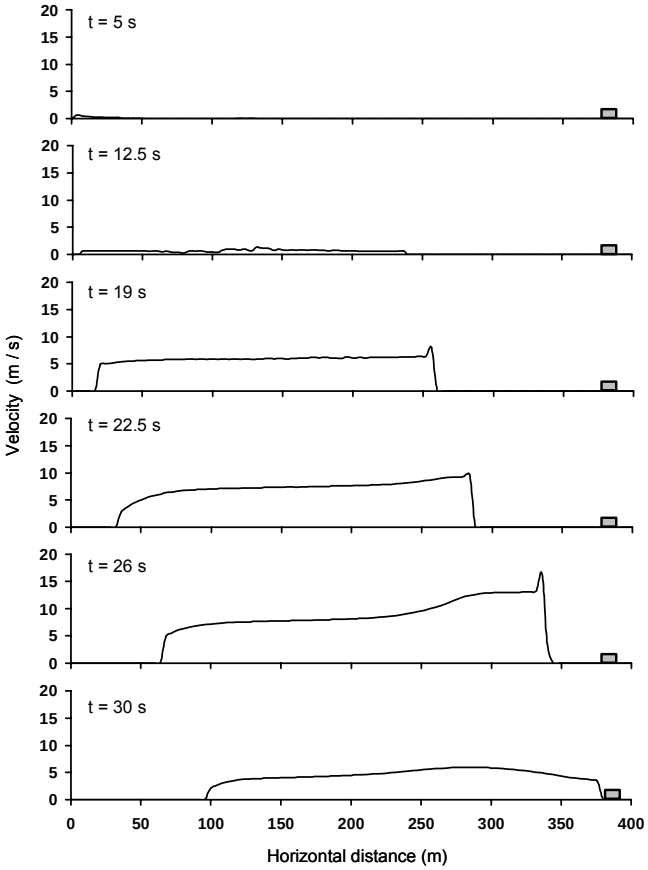

Fig. 15. Snapshots of the spatial distribution of velocity of the Higashi–Takezawa landslide. The school is indicated with the gray box

last 16 seconds of the analysis, the frontal edge of the landslide has already moved about 110 m. This is in satisfactory (at least qualitatively) agreement with reality. It is interesting to observe, that after its termination the landslide has a length of 160 m, that is approximately 2 times larger than its initial (before triggering) length. The expanding in nature evolution of the landslide, is also reflected in Fig. 18 which plots snapshots of the distribution of velocity. The velocity diminishes gradua and-
slide, t

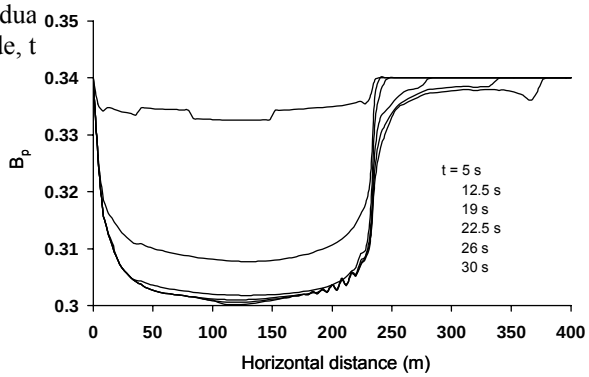

Fig. 16. Distributions of the breakage potential B_p along the sliding surface at various times, from t = 5 sec (top line), to t = 30 sec (bottom line)

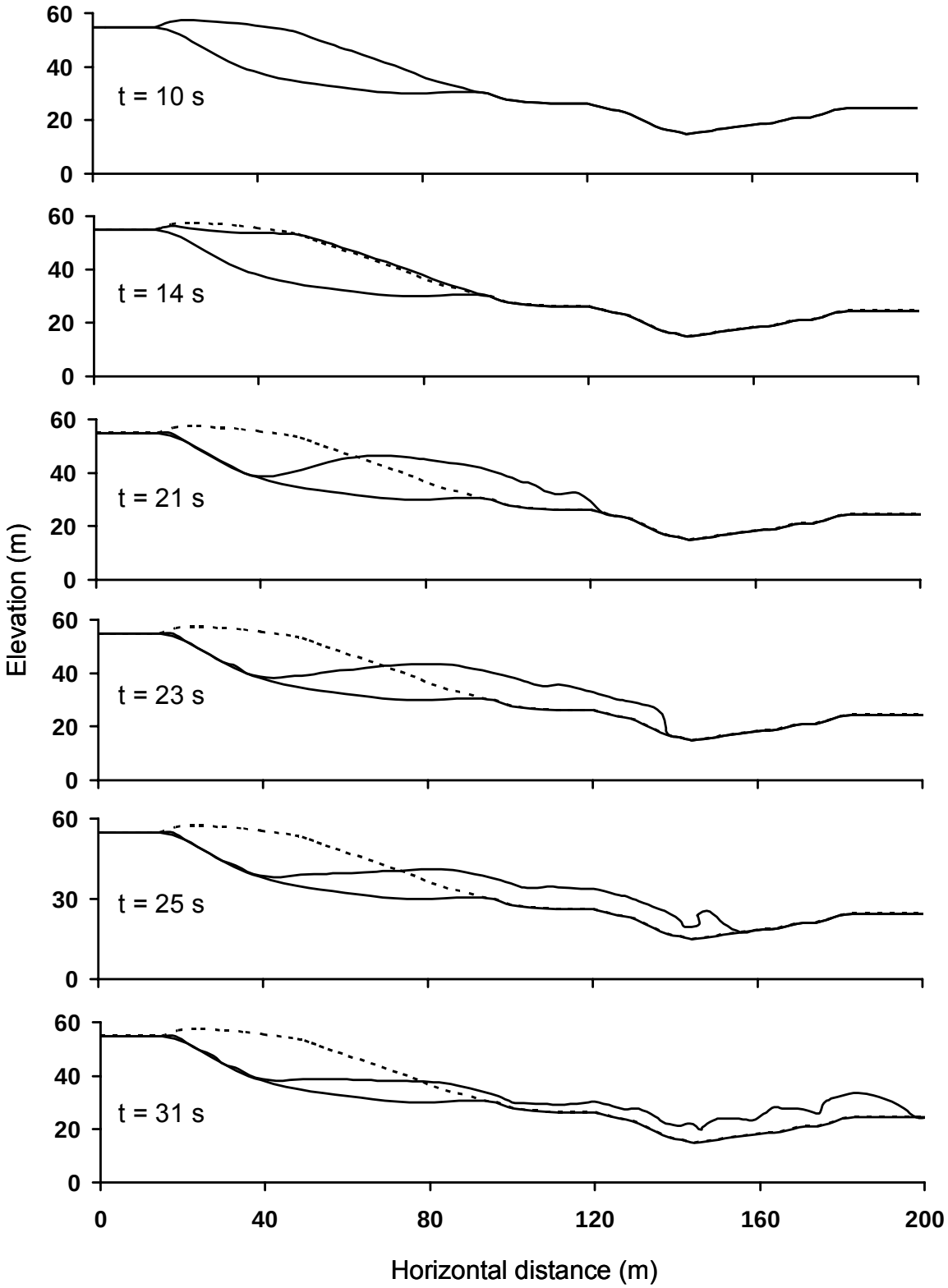

Fig. 17. Snapshot of the computed evolution of the Nikawa landslide. The initial ground surface is shown as dotted line

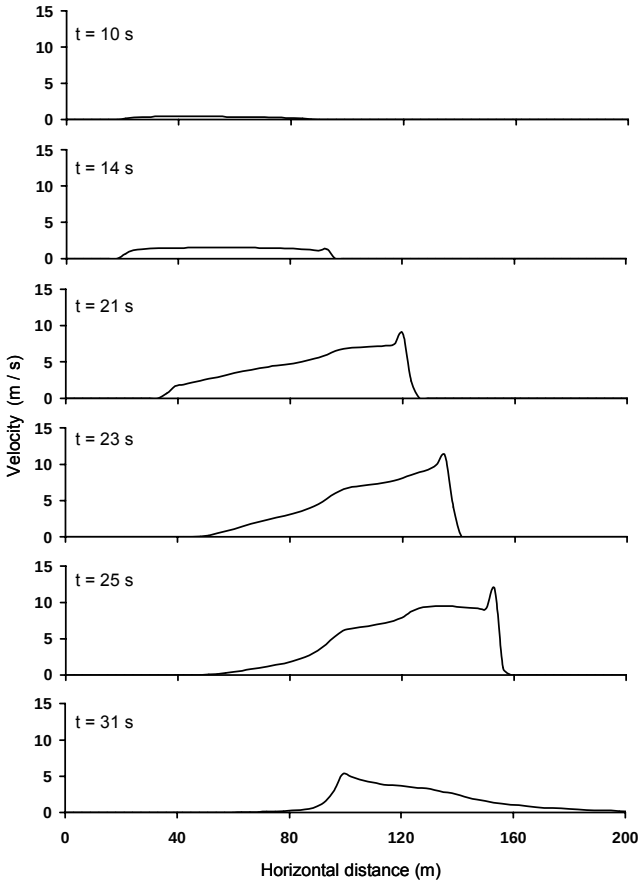

Fig. 18. Snapshots of the spatial distribution of velocity of the Nikawa landslide

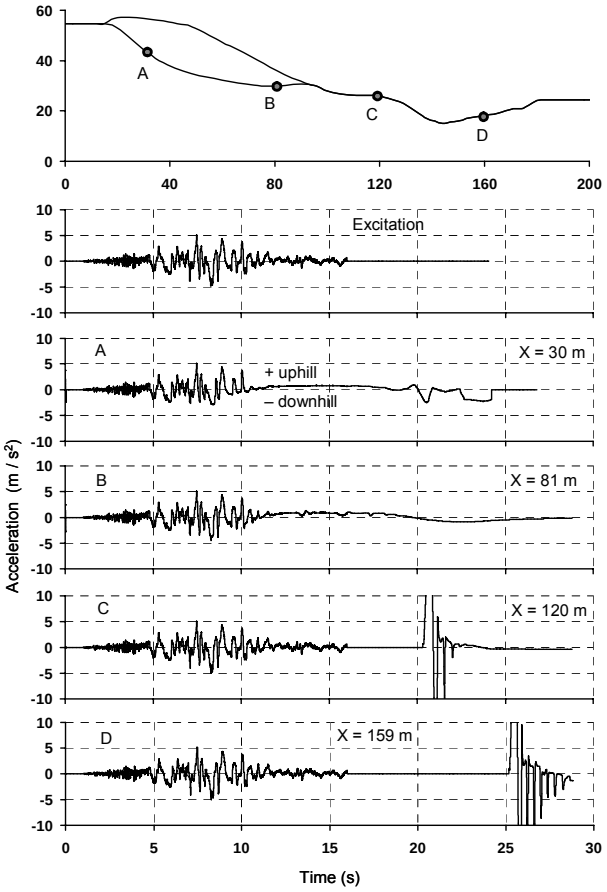

Fig. 19. Acceleration time histories at selected point along the sliding surface of the Nikawa landslide.

A more lucid explanation of the landslide evolution is given in Fig. 19, which plots the acceleration time histories at characteristic points along the sliding surface, and compares them with the excitation. At x = 30 m (point A) and x = 81 m (point B), the acceleration transmitted into the overlying soil wedge diminishes gradually, vanishing in the downhill direction. This arises from the material softening due to rapid development of high excess pore–water pressures within the shear band. Obviously, gravity is the predominant driving force at $t > 14$ sec.

By contrast to the gradual reduction of acceleration at points A and B, such reduction is not observed at points C and D. The propagation of excess pore–water pressure due to particle crushing has not yet reached those "distant" points. The abrupt increase in acceleration at $t \approx 21$ sec at point C, and at $t \approx 26$ sec at point D, signals the arrival of the frontal edge of the landslide.

CONCLUSIONS

In this paper a model was presented for seismic triggering, evolution and deposition of a landslide. The evolution of the landslide is modeled via an extended Savage–Hutter model coupled with the Mohr–Coulomb sliding law for the frictional deformation of the material within the shear band, and exploiting the concept of material softening due to grain crushing induced pore water pressures.

The capability of the model is investigated through prediction of two earthquake–induced catastrophic landslides. The Higashi–Takezawa la,ndslide in 2004, and the Nikawa landslide in 1995.

For the case of Higashi–Takezawa, three scenarios were analyzed regarding the location of the sliding surface and the susceptibility of sand to grain crushing: (a) shear band within the sand layer, with "stable" sand, (b) shear band within an assumed thin silt layer atop the siltstone, with "stable" sand, and (c) shear band within the sand layer, but sand susceptible to grain crushing. The residual displacement is calculated to be 0.65 m and 3.4 m for the first and second scenario, respectively. The observed approximately 100 m displacement of the

landslide, associated to a shear velocity of 16 m/sec (20 sec after the triggering), is only reproduced with the third scenario, despite the experimental fact that the residual friction angle of the silt [scenario (b)] was 13^o smaller than that of sand.

The following phases of the sliding process were shown to be reproduced with certain realism by the proposed model for landslide kinematics:

Material softening. Seismically induced shearing causes particle crushing inside the shear band, which in turn results in pore pressure generation and decreases the effective normal stress.

Landslide Triggering. This phase starts as soon as the pore water pressure inside the shear band reaches and surpasses a critical value, the gravitational driving force acting on the landslide mass dominates upon the resisting force due to hysteretic (Coulomb) friction at the base of the slide, and landsliding begins. It was shown that triggering occurs almost at the end of seismic shaking, when the motion of the mass has passed its peak, and not during the strong seismic excitation.

Post–failure behavior. During this phase the landslide is accelerating towards the deposition fan due to the action of gravity. Excess pore water pressure continuous to increase but the rate of its generation diminishes gradually, because the extra pore pressure cannot increase more than the initial effective stress, or the effective normal stress has decreased to a certain value under which grain crushing does not further take place.

Deposition and Termination of the Landslide. Deceleration and finally termination of the landslide occurs primarily due to the influence of negative inclination of the basal topography. For example, in the case of Higashi Takezawa, the downhill bank of the river restricted the motion of the depositing soil mass, which in turn blocked the flow of the incoming trailing part of the slide. Being pushed from both sides, the depositing soil mass came to rest. The hydraulic resisting force at the base of the slide is also a major stabilizing factor contributing positively to the deceleration of the landslide.

ACKNOWLEDGMENTS

The research for this paper was funded by the EU sixth Framework Program: Integrated R&D Project of the EC "Risk Mitigation of Earthquakes and Landslides", Research Project LESSLOSS, Contract number: GOCE-CT-2003-505448.

REFERENCES

Bouc R. [1971] "Modele mathematique d' hysteresis", *Acustica*, Vol. 21, pp.16-25

Committee of Earthquake Engineering [1996] "The 1995 Hyogo-Ken Nambu earthquake–Investigation into damage to civil engineer structures", *Japan Society of Civil Engineers*.

Earthquake Engineering Research Institute [1995] "The Hyogo-Ken Nambu earthquake, January 17, 1995", *Preliminary EERI Reconnaissance Report*.

Gerolymos N, Gazetas G [2004] "Constitutive Model for 1-D Cyclic Soil Behavior Applied to Seismic Analysis of Layered Deposits", *Soils and Foundations*, Vol. 45, No 3, pp. 147–159.

Gerolymos N., Gazetas G [2007a] "Seismic Triggering, Evolution and Deposition of Massive Landslides: The Case of Higashi–Takezawa (2004)", *Proceedings of the 4th International Conference on Earthquake and Geotechnical Engineering (ICEGE)*, Thessaloniki, Greece, June 25–28, (in Cd).

Gerolymos N and Gazetas G [2007b] "A Model for Grain Crushing Induced Landslides − Application to Nikawa, Kobe 1995", *Soil Dynamics and Earthquake Engineering*, Vol. 27, pp. 803–817.

Gerolymos N, Vardoulakis I and Gazetas G [2007] "A thermo-poro-viscoplastic shear band model for triggering and evolution of catastrophic landslides. *Soils and Foundations*, Vol. 47, No. 1, pp. 11-25.

Gray J.M.N.T., Wieland M., Hutter K [1999] "Gravity driven free surface flow of granular avalanches over complex topography", *Proc. R. Soc. London A*, Vol. 455, pp. 1841-1874.

Hardin B [1985] "Crushing of Soil Particles" *Journal of Geotechnical Engineering*, Vol. 111, No. 10, pp. 1177-1192.

Iverson R. M., Delinger R. P. [2001] "Flow of variably fluidized granular masses across three-dimensional terrain. 1. Coulomb mixture theory" *J. Geophys. Res. B*, Vol. 106, pp. 537-552.

Japanese Geotechnical Society [1996] "Geotechnical aspects of the January 17, 1995 Hyogoken-Nambu earthquake", *Soils and Foundations*, Special Issue 1996.

Kallou P, and Gazetas G [2001] "Dynamic Analysis of Nikawa Landslide", *Proceedings of the 4th Hellenic Conference on Geotechnical and Geoenvironmental Engineering*, Athens, Vol. 2, pp. 171-178.

Kokusho T [2000] "Mechanisms for water film generation and lateral flow in liquefied sand layer", *Soils and Foundations*, Vol. 40, No. 5, pp. 99-111.

Kokusho T, Ishizawa T [2005] "Energy approach to slope failures and a case study during 2004 Niigata–ken Chuetsu earthquake", *Proceedings of Geotechnical Earthquake Engineering Satellite Conference Osaka*, Japan, ISSMGE, pp. 255-262.

Koseki J., Sasaki T., Wada N., Hida J., Endo M., Tsutsumi Y. [2006] "Damage to earth structures for national highways by the 2004 Niigata-Ken Chuetsu earthquake", *Soils and Foundations*, Vol. 46, No. 6, pp. 739-750.

Newmark, N M. [1965] "Effect of earthquakes on dams and embankments" *Géotechnique*, Vol.15, pp. 139–160.

Pudasaini S P, Hutter K [2003] "Rapid shear flows of dry granular masses down curved and twisted channels", *J. Fluid Mech*., Vol. 495, pp. 193-208.

Sato T. [1996] "Estimation of peak acceleration in the severely damaged area during the 1995 Hyogo-Ken Nanbu earthquake", *Soils and Foundations*, Special Issue, pp. 35-44.

Sassa K, Fukuoka H, Wang F, Wang G. [2005] "Dynamic properties of earthquake-induced large-scale rapid landslides within past landslide masses", *Landslide*, Vol. 2, pp. 125-134.

Sassa K. [2005] "Landslide disasters triggered by the 2004 Mid-Niigata Prefecture earthquake in Japan", *Landslides*, Vol. 2, pp. 135-142.

Sassa K, Fukuoka H, Scarascia-Mugnozza G, Evans S. [1996] "Earthquake induced Landslides: distribution, motion and mechanisms", *Special Issue of Soils and Foundations, Japanese Geotechnical Society*, pp. 53-64.

Sassa K. [1995] "Keynote lecture: Access to the dynamics of landslides during earthquakes by a new cyclic loading high-speed ring shear apparatus", *Proceedings 6th International Symposium on Landslides 1992, In "Landslides"*. Balkema, Vol. 3, pp. 1919-1939.

Sassa K. [1994] "Development of a new cyclic loading ring shear apparatus to study earthquake–induced–landslides", *Report for Grant-in-Aid for Development Scientiffic Research by the Ministry on Education, Science and Culture*, Japan (Project No. 03556021), pp. 1-106.

Toyota H., Wang J., Kouichi N., Sakai N. [2006] "Evaluation of natural slope failures induced by the 2004 Niigata-Ken Chuetsu earthquake", *Soils and Foundations*, Vol. 46, No. 6, pp. 727-738.

Tsukamoto Y, Ishihara K. [2005] "Residual strength of soils involved in earthquake–induced landslides", *Proceedings of Geotechnical Earthquake Engineering Satellite Conference, Osaka, Japan, 10 September 2005*, Performance Based Design in Earthquake Geotechnical Engineering: Concepts and Research, ISSMGE, pp. 117-123.

Wen Y.-K. [1976] "Method for random vibration of hysteretic systems", *Journal of Engineering Mechanics, ASCE*, Vol. 102, pp. 249-263.